

# Improving tensile and fatigue properties of Sn–58Bi/Cu solder joints through alloying substrate

QingKe Zhang, HeFei Zou, and Zhe-Feng Zhang<sup>a)</sup>

*Shenyang National Laboratory for Materials Science, Institute of Metal Research, Chinese Academy of Sciences, Shenyang 110016, People's Republic of China*

(Received 27 August 2009; accepted 5 November 2009)

To eliminate the Bi segregation and interfacial embrittlement of the SnBi/Cu joints, we deliberately added some Ag or Zn elements into the Cu substrate. Then, the reliability of the SnBi/Cu–X (X = Ag or Zn) solder joints was evaluated by investigating their interfacial reactions, tensile property, and fatigue life compared with those of the SnBi/Cu and SnAg/Cu joints. The experimental results demonstrate that even after aging for a long time, the addition of the Ag or Zn elements into the Cu substrate can effectively eliminate the interfacial Bi embrittlement of the SnBi/Cu–X joints under tensile or fatigue loadings. Compared with the conventional SnAg/Cu joints, the SnBi/Cu–X joints exhibit higher adhesive strength and comparable fatigue resistance. Finally, the fatigue and fracture mechanisms of the SnBi/Cu–X solder joints were discussed qualitatively. The current findings may pave the new way for the Sn–Bi solder widely used in the electronic interconnection in the future.

## I. INTRODUCTION

The toxicity of the Pb presents a major health hazard, many lead-free solder alloys have been proposed as alternatives in the electronic packaging field.<sup>1,2</sup> Among the potential alternatives, the Sn–58Bi eutectic alloy had once been recognized as a promising substitute because its mechanical and physical properties are comparable to those of the Sn–37Pb eutectic solder alloy.<sup>3,4</sup> It is particularly attractive in the low-temperature soldering field, which refers to soldering at temperatures between 170 and 200 °C, and is superior in alleviating the thermal damage in a package.<sup>5,6</sup> It has been reported that the Sn–58Bi alloy has higher shear strength and superior creep resistance than those of the Sn–Pb solder at temperatures between 20 and 70 °C.<sup>4</sup> The Sn–58Bi solder is also distinguished by its excellent mobility in the molten state, especially zero shrinkage upon solidification,<sup>3</sup> and the wettability on Cu substrate is reliable according to its surface tension in air and wetting force on bare Cu coupons.<sup>5</sup> In addition, the Bi element is widely used as an alloying agent to enhance the strength of the other series of lead-free solders.<sup>1–3</sup>

Although there are a lot of advantages for the Sn–Bi alloy, the potential Bi segregation at the Cu<sub>3</sub>Sn/Cu interface of SnBi/Cu solder joints during thermal aging process becomes a fatal drawback.<sup>7,8</sup> Because of the interfacial embrittlement induced by Bi segregation, the

adhesive strength and fatigue resistivity of the long-term aged Cu/Cu–Sn intermetallic (IMC) interface are severely deteriorated, and the reliability of the SnBi/Cu joint becomes questionable. The predominant use of Cu metallization in printed circuit boards (PCBs)<sup>2,8</sup> has greatly limited the application of the Sn–Bi solder in electronic assembly. Therefore, to heal or alleviate the interfacial embrittlement, it is necessary to eliminate the Bi segregation at the long-term aged SnBi/Cu joints. In recent years, there have been some studies in an attempt to enhance the mechanical properties of the Sn–58Bi/Cu interface. Zhu et al.<sup>9</sup> had reported that an electrodeposition of a thin Ag layer on Cu substrate can restrain the Bi segregation at the interface. In addition, electrodeposition of Ni layer on Cu substrate had also been investigated by Liu and Shang.<sup>10</sup> However, the electrodeposition technology increases the cost in electronic assembly and does not really heal the embrittlement of the SnBi/Cu interface. New techniques to eliminate the interfacial Bi segregation still need to be further investigated.

For this purpose, we tried to restrain the interfacial Bi segregation by adding some alloy elements into the Cu substrate; the alloying elements may change the diffusion processes of the Bi atoms and promote it to diffuse into the Cu alloy substrate. The experimental results confirmed that a small addition of some elements (e.g., Ag, Al, Zn, or Sn) into the Cu substrate can completely eliminate the interfacial Bi segregation at the reflowing temperature of 200 °C,<sup>11</sup> which provides a potential technique to heal the interfacial embrittlement of the

<sup>a)</sup>Address all correspondence to this author.

e-mail: zhfzhang@imr.ac.cn

DOI: 10.1557/JMR.2010.0035

long-term aged SnBi/Cu joints and is of great importance for popularization of the Sn–Bi solder. In this paper, the interfacial morphology, tensile and fatigue properties, and the corresponding fracture behaviors of the Sn–58Bi/Cu–2.5Ag and Sn–58Bi/Cu–10Zn solder joints aged for different times are investigated systematically. Then they are compared with those of the SnBi/Cu solder joints to further check the validity of the alloying in improving the interfacial reliability. In addition, the adhesive properties of the SnBi/Cu–X solder joints are also compared with those of other series of solders, i.e., the Sn–4Ag/Cu and Sn–37Pb/Cu solder joints. The evolution of the interfacial microstructure, tensile properties, and fracture mechanism of the Sn–58Bi bulk alloy during aging process are also investigated as a reference and compared with those of the Sn–4Ag solder. Based on the aforementioned results and observations, the reliability of the SnBi/Cu–X joints are evaluated and the application prospect of the Sn–Bi solder alloy is proposed.

## II. EXPERIMENTAL PROCEDURE

The Cu substrate material used in this study was prepared from oxygen-free-high-conductivity (OFHC) Cu of 99.999% purity by vacuum smelting operated in a vacuum furnace with the maximum heating temperature of 1600 °C. The Cu was first melted, kept at 1200 °C for 2 h, and then cooled with the furnace. The Cu–2.5Ag (at.%) and Cu–10Zn (at.%) alloy substrate materials were prepared from the same Cu raw material and high-purity Zn and Ag by the same smelting process. Observations of optical microscope show that all the substrate materials have coarse grains. The Sn–58Bi (wt%) solder alloy used in this study was fabricated by smelting high-purity (>99.99%) tin and bismuth in vacuum at 800 °C for 2 h. The Sn–4Ag solder was prepared from high-purity (>99.99%) tin and silver by the same melting process. At moderate cooling rates, the microstructure of the Sn–58Bi eutectic alloy is lamellar, with degenerated material at the boundaries of the eutectic grains, and the Sn–4Ag (wt%) alloy is composed of proeutectic platelike  $\text{Ag}_3\text{Sn}$  intermetallics and a eutectic structure of Sn and  $\text{Ag}_3\text{Sn}$  based on the Sn–Ag binary phase diagram.<sup>2,4</sup>

The plates of substrate materials were spark-cut into blocks first, and the ends to be soldered were carefully polished with a diamond polishing agent. Before soldering, a soldering paste was first dispersed on the selected area of the polished surface, then a solder alloy sheet was placed on the paste to ensure sufficient wetting reaction. The graphite plates were clamped on the sides of the Cu and Cu–X alloy samples with the solder paste to prevent the outflow of the molten solder. For the Sn–58Bi solder, the prepared samples were fixed in an oven with a constant temperature of 200 °C for 60 s after melting of solder and then were cooled down in air.

Some selected samples were isothermally aged at 120 °C for 7, 13, and 20 days (also 5 and 10 days for the SnBi/Cu samples), respectively. The reflowing temperature of the Sn–4Ag/Cu solder joints was 260 °C, kept for 180 s after melting of solder, and some selected samples were aged at 180 °C for different times. After that, both the as-soldered and aged samples were spark-cut into tensile and fatigue specimens, and the side surfaces were ground and carefully polished for observations of the interfacial morphologies and deformation behaviors at the solder/substrate interfaces. The Sn–58Bi and Sn–4Ag bulk solder alloys were cut into standard samples and underwent the same aging process with the solder joints. The geometry and size of all the specimens are illustrated in Fig. 1.

Both the tensile and fatigue tests were carried out with Instron 8871 and E1000 fatigue testing machines (Norwood, MA) at room temperature in air. Tensile tests were performed under a cross-beam speed of  $3.75 \times 10^{-3}$  mm/s to obtain a strain rate of about  $1.25 \times 10^{-4} \cdot \text{s}^{-1}$ . The stress-controlled fatigue tests were performed under a symmetrical sinusoid with a frequency of 2 Hz. The stress ratio ( $R$ ), defined as the ratio of the stress amplitude ( $\sigma_a$ ) to the tensile strength of the samples ( $\sigma_b$ ), was in the range of 0.4 to 0.8, varied for different solder joints. The cross-section and fracture surfaces of the specimens were observed in a LEO Supra 35 field emission scanning electron microscope (SEM) with energy-dispersive x-ray (EDX) spectroscopy (Carl Zeiss, Germany) to reveal the tensile and fatigue fracture mechanisms.

## III. RESULTS AND DISCUSSION

### A. Evolution of interfacial morphology during aging process

The interfacial morphologies of the SnBi/Cu joints are shown in Fig. 2. For the as-soldered joint exhibited in Fig. 2(a), an IMC layer of about 1  $\mu\text{m}$  thick was observed between the Cu substrate and SnBi solder. Energy-dispersive x-ray spectroscopy (EDX) analysis indicated that the layer is  $\text{Cu}_6\text{Sn}_5$  intermetallic compound. Compared with the previous reports on the

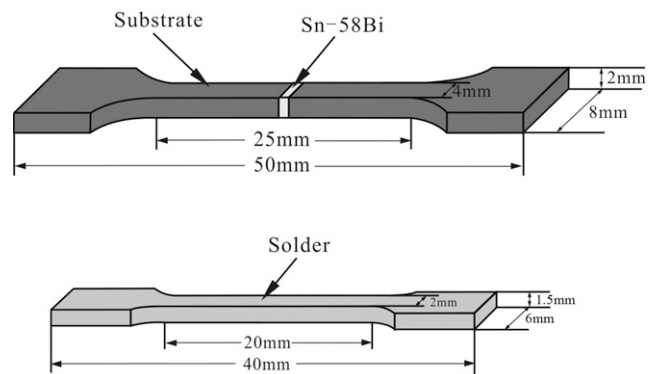


FIG. 1. Shape and dimensions of the tensile and fatigue specimens.

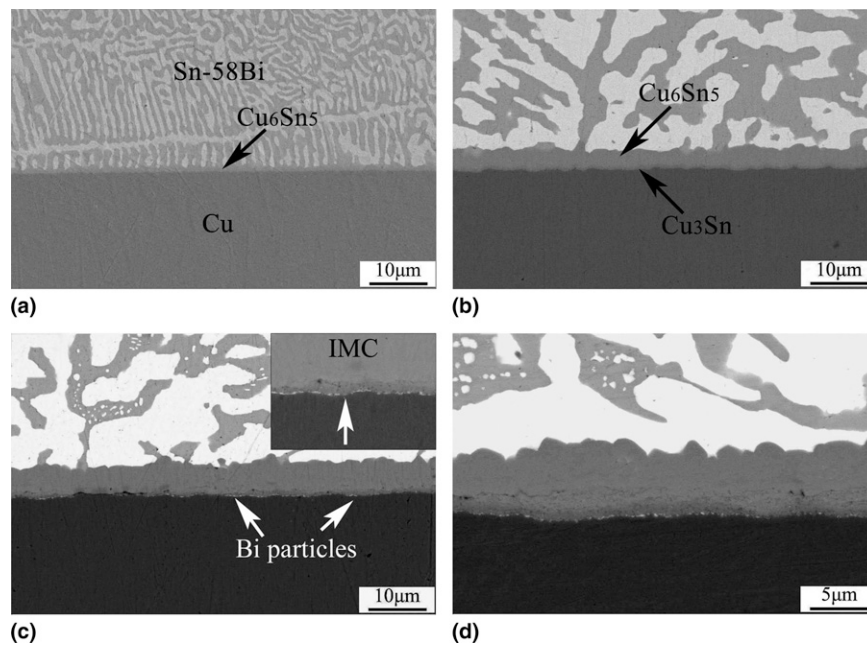


FIG. 2. Interfacial morphologies of Sn–58Bi/Cu solder joints. (a) As-soldered and (backscattered electron images) aged for (b) 5 days, (c) 10 days, and (d) 13 days.

SnBi/Cu interface,<sup>7,11</sup> it was found that the interfacial IMC layer was relatively thin, which may be attributed to the shorter reflowing time (60 s). After aging at 120 °C for 5 days, the IMC layer became evidently thick, and a thin  $\text{Cu}_3\text{Sn}$  layer was observed between the Cu substrate and the  $\text{Cu}_6\text{Sn}_5$  layer, as shown in its backscattered electron image [see Fig. 2(b)]. Meanwhile, noticeable coarsening of the microstructure of the Sn–Bi eutectic was observed, which may induce a change in the mechanical properties of the solder alloy. The interfacial morphologies of the samples aged for 10 and 13 days are shown in Figs. 2(c) and 2(d), respectively. It is obvious that the IMC thickness keeps increasing with increasing aging time, while the alteration of the interfacial morphology was slight. Similar to earlier reports,<sup>7–9</sup> discontinuous Bi particles (the bright spots) were also observed at these long-term aged IMC/Cu interfaces, which mainly came from the Bi diffusion of the SnBi solder through the IMC layers during soldering and aging processes.<sup>11</sup> Because the Cu–Bi system is completely immiscible,<sup>12–14</sup> the diffusion of Bi atoms into the pure Cu substrate should be extremely difficult, and the Bi atoms can easily segregate at the  $\text{Cu}_3\text{Sn}/\text{Cu}$  interface to form the particles. In addition, compared with the microstructure of the SnBi solder in Figs. 2(b)–2(d), the solder shows little coarsening during the later stage of aging, indicating that coarsening of the solder alloy only occurred at the early stage of aging.

The interfacial morphologies of the as-soldered SnBi/Cu–X solder joints are similar to that of the SnBi/Cu samples, while those of the aged SnBi/CuAg and SnBi/CuZn joints are a bit different, as shown in Fig. 3. It

is obvious that though the evolution process of the SnBi/Cu–X interfaces during aging is similar to that of the SnBi/Cu interface, Bi segregation was not observed at the  $\text{Cu}_3\text{Sn}/\text{Cu}$ –X interface even after aging for 20 days. The observations provide direct evidence that the addition of Ag or Zn elements to the Cu substrate can eliminate the Bi segregation of the long-term aged SnBi/Cu interface. In fact, though the Bi atoms will still diffuse to the IMCs/CuAg interface during the aging process, it has been reported that the replacement of Ag atoms by Bi atoms makes the Cu–Ag system more stable compared with the binary Cu–Ag alloy<sup>15</sup>; thus, the Bi atoms will diffuse into the Cu–Ag alloy to form a more stable CuAgBi ternary phase. The mechanism in the SnBi/CuZn joints may be similar. Another significant finding is that the interfacial IMC thicknesses at the SnBi/Cu and SnBi/Cu–X interfaces aged for the same time are a little different. As exhibited in Fig. 4, although the IMC thicknesses of both the SnBi/Cu and the SnBi/Cu–X interfaces increase linearly with the square root of aging time, the interfacial IMC thicknesses of the SnBi/Cu–X solder joints are a bit lower than that of the SnBi/Cu interface at the same aging time. Thus, such a difference may induce a different tensile strength. Previous results indicated that the growth kinetics of interfacial Cu–Sn IMCs can be expressed by the following one-dimensional empirical equation<sup>16–18</sup>:

$$\delta = \delta_0 + \sqrt{Dt} \quad , \quad (1)$$

where  $\delta$ ,  $\delta_0$ ,  $D$ , and  $t$  are the thicknesses of IMC at time  $t$ , the initial thicknesses of IMC, the diffusion coefficient,

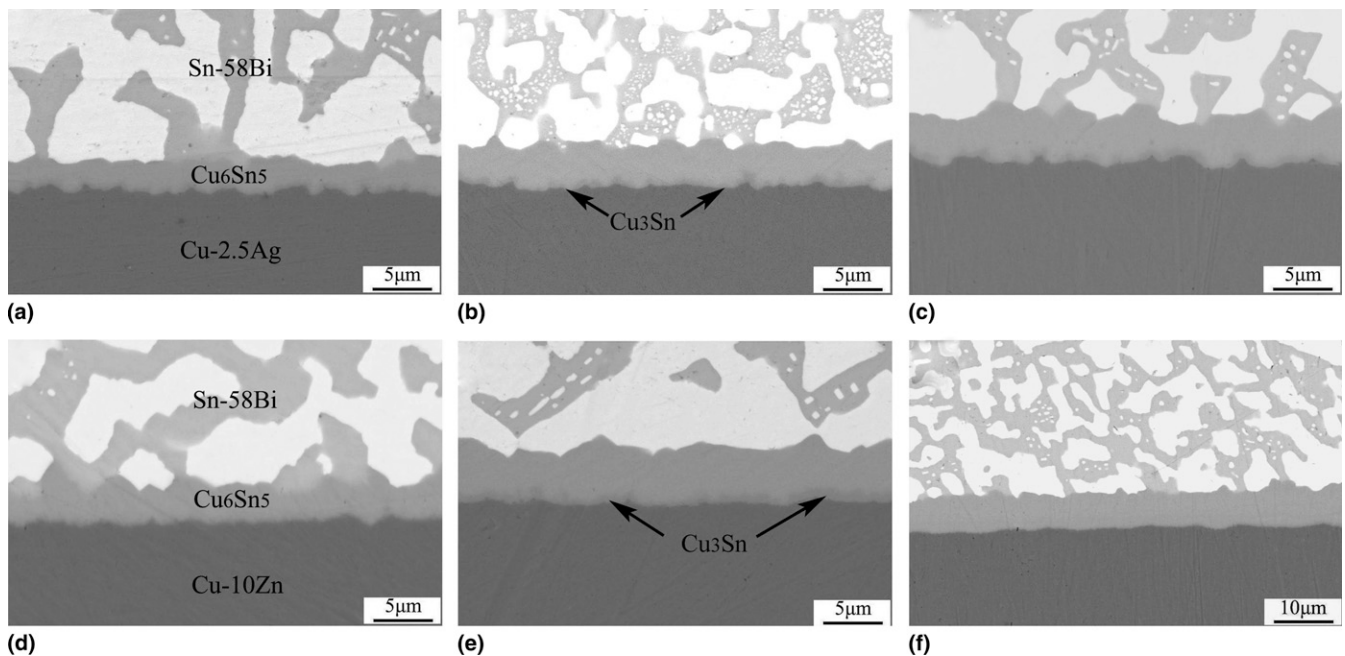


FIG. 3. Interfacial morphologies (backscattered electron image) of Sn–58Bi/Cu–2.5Ag solder joints aged for (a) 7 days, (b) 13 days, (c) 20 days, and Sn–58Bi/Cu–10Zn solder joints aged for (d) 7 days, (e) 13 days, and (f) 20 days.

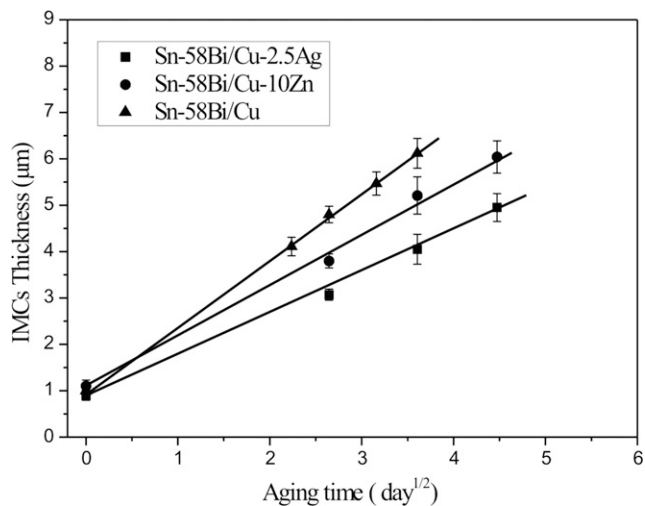


FIG. 4. Dependence of total IMC thickness of the SnBi/Cu and SnBi/Cu-X interfaces on the aging time.

and the aging time. The values  $D$  were calculated to be  $2.33 \times 10^{-17}$ ,  $9.49 \times 10^{-18}$ , and  $1.41 \times 10^{-17}$  m<sup>2</sup>/s for the SnBi/Cu, SnBi/Cu–2.5Ag, and SnBi/Cu–10Zn joint interfaces, respectively. Considering the influence of the microstructure of substrate material on its diffusion process, the difference in the diffusion coefficient may be attributed to the types and quantity of the additive elements because they may change the atomic arrangement and lattice parameter of the substrate material. Influence of alloy element addition on the diffusion process of the substrate materials is discussed in detail elsewhere.<sup>19</sup>

The aforementioned observation results have confirmed that the Bi segregation in the SnBi/Cu–X solder joints has been completely eliminated. However, previous studies revealed that the adhesive strength of the solder joints decreased with increasing interfacial IMC thickness.<sup>20–22</sup> Thus, the aging process might slightly deteriorate the adhesive strength of the SnBi/Cu–X joints. In addition, discontinuous interfacial Bi-rich phase was formed at the long-term aged SnBi/Cu–X interfaces because of the preferential consumption of Sn during the growth process of the interfacial IMCs,<sup>23</sup> which may also decrease the interfacial strength as the Bi-rich phase is rigid and brittle.<sup>8</sup>

## B. Tensile behaviors of Sn–58Bi and Sn–4Ag alloys

The tensile property of the Sn–58Bi solder was also investigated in this study to make a more comprehensive evaluation. Figure 5 shows the tensile stress–strain curves of the air-cooled and isothermally aged Sn–58Bi samples; the curves of the Sn–4Ag samples aged at 180 °C for different times are also given for comparison. It is notable that all the stress–strain curves are similar in shape: after the elastic deformation, the flow stress reaches its peak shortly after yielding because of the low strain-hardening rate, and then decreases with increasing strain. Finally, all the samples failed in a ductile mode and the necking is obvious. The elongation of the aged samples is higher, while its yield strength is a bit lower than that of the air-cooled sample, which contributes to the coarsening of solder grains during the aging process. It is interesting to find that both the tensile

strength and elongation of Sn–58Bi solder are all much higher than those of the Sn–4Ag solder, because the Bi-rich phase in the Sn–Bi eutectic structure is hard and brittle and will decrease the deformation behaviors of the solder.<sup>8</sup> In fact, it has been reported that the elongation percentage of the Sn–58Bi alloy is in the range of 20–150%, varying with testing temperature and strain rate.<sup>24,25</sup> From the aforementioned results and discussions, it can be concluded that Sn–58Bi bulk solder has high tensile strength and good elongation at room temperature and low strain rate.

The variation of the ultimate tensile strengths (UTS) of the Sn–58Bi and Sn–4Ag bulk solder alloys with the aging times is shown in Fig. 6. It is found that the average UTS (~50 MPa) of the Sn–58Bi solder is much higher than that (~20 MPa) of the Sn–4Ag solder. In addition, the UTS of the two solder alloys decreases

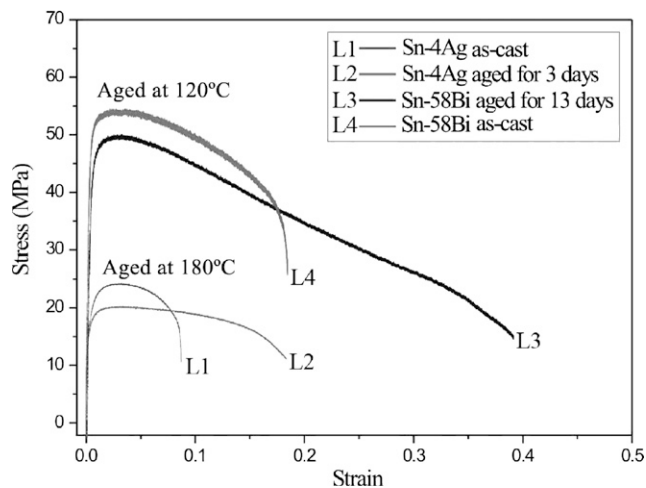


FIG. 5. Tensile stress–strain curves of the Sn–4Ag and Sn–58Bi bulk solder alloys.

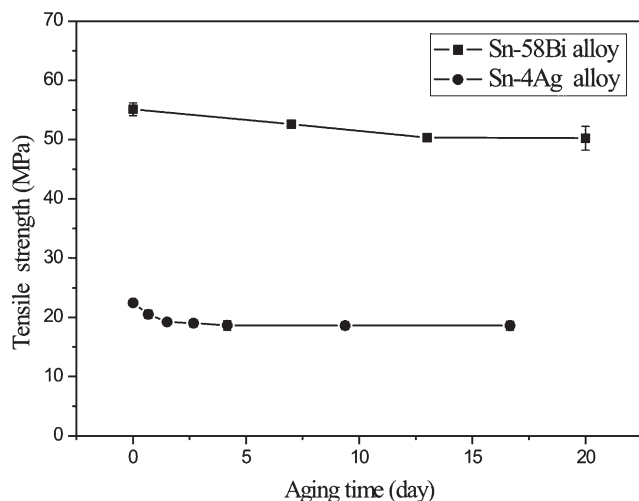


FIG. 6. Variation of tensile strengths of the Sn–58Bi alloy aged at 120 °C and Sn–4Ag alloy aged at 180 °C with the aging times.

only a little at the early stage of aging and remains nearly constant during the later aging process. As mentioned previously, because obvious coarsening of the solder grains only occurred at the early stage of aging, the variation of the microstructure of solder is small during the later stage of aging. As the tensile strength of the two solders decreases slightly, the variation of tensile strength of the solder joints during aging process may be mainly attributed to the evolution of the solder/substrate interfacial structure.

### C. Adhesive strength and fracture mechanism

#### 1. Tensile strength of solder joints

The UTS of the solder joints aged for different times is shown in Fig. 7. It is clear that the tensile strengths of all the solder joints did not obviously decrease with increasing aging time except for the SnBi/Cu solder joint. As the tensile strengths of the solders themselves only have a slight decrease during the aging process, the decrease should be controlled by evolution of the solder/substrate interfaces. The UTS of the SnBi/Cu solder joint is still high before aging for 7 days, but drops dramatically after aging for more than 7 days. The SnBi/Cu joints aged for 13 days have become brittle, having undergone a ductile-to-brittle transition, and are compared with their tensile fracture morphologies in Sec. III. C. 2. Such a transition is consistent with former reports.<sup>7–10</sup> Compared with the SnBi/Cu joints, the tensile strengths of the SnBi/CuAg and SnBi/CuZn solder joints did not show a dramatic drop even after a longer aging time (up to 20 days), indicating that the interfacial embrittlement of the long-term aged SnBi/Cu solder joints has been eliminated. Besides, the tensile strengths of the two SnBi/Cu–X solder joints are higher than that of the SnBi/Cu solder joint even before the embrittlement occurs. Therefore, it is predicated that the addition

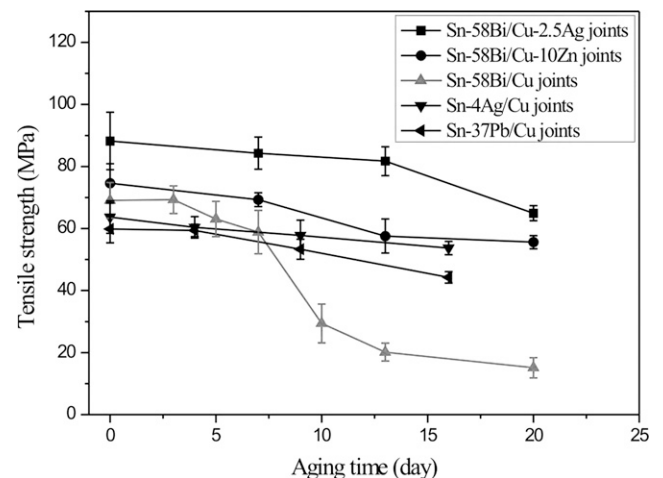


FIG. 7. Evolution of tensile strengths of the SnBi/Cu, SnBi/Cu–X, SnAg/Cu, and SnPb/Cu solder joints during aging process.

of Ag or Zn elements into Cu substrate not only eliminated the interfacial Bi embrittlement of the SnBi/Cu joint, but also improved the tensile strength. In addition, the tensile strengths of the Sn–4Ag/Cu and the Sn–37Pb/Cu solder joints aged at 160 °C for different times are a bit lower than those of the SnBi/Cu–X joints,<sup>26,27</sup> as exhibited in Fig. 7. The tensile fracture mechanism of the SnBi/Cu and SnBi/Cu–X solder joints in combination with the fracture morphologies is discussed in more detail in Sec. III. C. 2.

## 2. Tensile fracture behaviors

For all the SnBi/Cu and SnBi/Cu–X tensile samples, although the strain rate is low and the deformation of the substrate material is obvious, the plastic deformation of the solder is small. Typically, the solder joints fracture next to the solder/substrate interface, as shown in Fig. 8. Although the ductility of the Sn–58Bi solder is good at

the current strain rate, there is no obvious plastic deformation or necking in solder because the tensile strength of the solder joints is only a little higher than the yield strength of the SnBi solder. It seems that the solder joints fractured at the interface prior to the sufficient plastic deformation of the solder. As the yield strength of the substrate materials is even lower than that of the Sn–Bi solder, the transverse shrinkage of the solder alloy is less than that of the substrate material during tensile deformation. The mismatch in transversal shrinkage induces a shear stress along the SnBi/Cu–X interface. When the yield strength of the substrate material is higher, as the mismatch between the substrate and the solder is less serious, the adhesive strength of the solder joint should be higher. Accordingly, the higher yield strength of the Cu–2.5Ag and Cu–10Zn alloys than Cu may be the main reason why the SnBi/Cu–X solder joints exhibit higher tensile strength than the SnBi/Cu joints. In general, the mechanical property of the soldering interface is much more influential to the adhesive strength than that of the solder alloy itself in the SnBi/Cu–X solder joints.

The tensile fracture surfaces of the as-soldered SnBi/Cu–X and SnBi/Cu joints are similar and are described in the next paragraph. The fracture surfaces of the long-term aged SnBi/Cu solder joints are essentially different from those of the as-soldered ones. Figure 9 employs the SnBi/Cu samples aged for 10 days as an example. The fracture surface is composed of bright and dark regions, as shown in Fig. 9(a). At the high magnification shown in Fig. 9(b), the bright region is found to be a thin layer of cracked solder, with Cu<sub>6</sub>Sn<sub>5</sub> IMC grains under it, while the dark area is the exposed Cu substrate. The

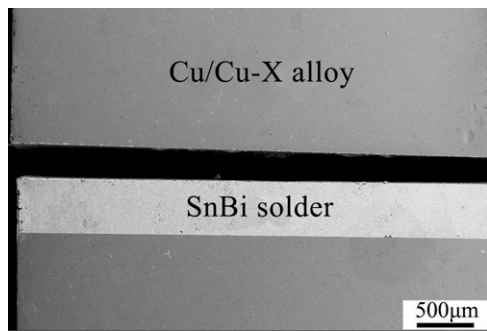


FIG. 8. Macroscopic side-surface images of cracked SnBi/Cu and SnBi/Cu–X joint samples.

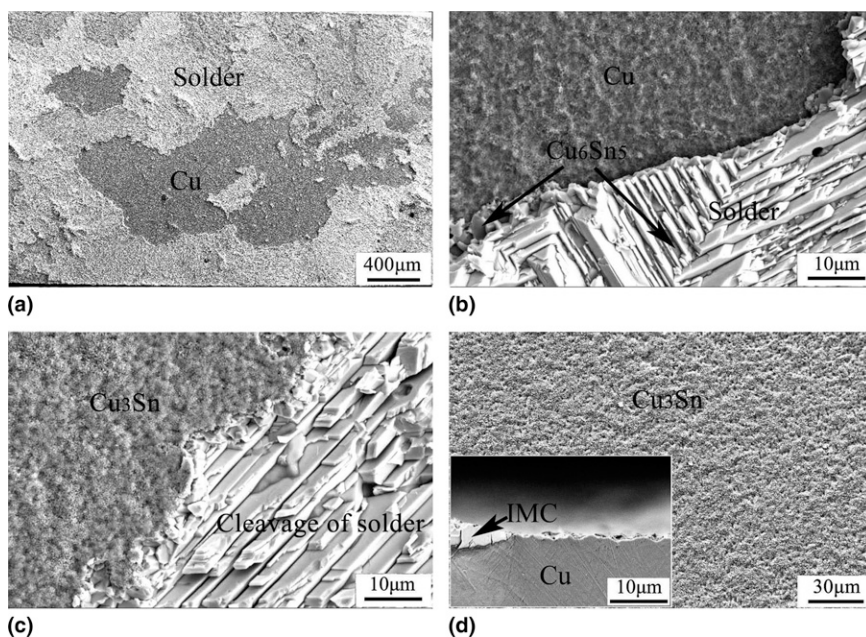


FIG. 9. Tensile fracture surfaces of the long-term aged SnBi/Cu samples. (a) Macroscopic morphology. (b, c) Microscopic morphology of the fracture surfaces. (d) Microscopic morphology and side surface of brittle fracture region.

opposing crack surface in Fig. 9(b) is shown in Fig. 9(c), in which the dark region is composed of small IMC grains, identified to be  $\text{Cu}_3\text{Sn}$  phase by EDX analysis. Besides, there are some voidlike spots [see Fig. 9(d)] at the fracture surface, which were considered to be Kirkendall voids induced by the Bi segregation.<sup>28</sup> The side surface of the brittle fracture region is also shown in Fig. 9(d), in which little IMC is left at the fractured interface. Figures 9(b)–9(d) show that the samples fractured at the Cu/ $\text{Cu}_3\text{Sn}$  interface at the dark region, while inside the solder close to the solder/ $\text{Cu}_6\text{Sn}_5$  interface at the bright region. The dark region is considered to be the trace of the interfacial embrittlement induced by the Bi segregation and the voids,<sup>7</sup> and its percentage will keep increasing with increasing aging time, making the SnBi/Cu solder joints more brittle.

The tensile fracture surfaces of the as-soldered and aged SnBi/CuAg and SnBi/CuZn solder joints are similar. Figure 10 shows the fracture surfaces of the SnBi/CuAg joints as an example; the side surfaces are also given out as an appendant. The fracture surface of the as-soldered samples is rough and covered by cracked solder alloy, as shown in Fig. 10(a). In the microscopic view, it can be seen that fracture mainly occurred along some facets of solder grains [see Fig. 10(b)], showing a typical cleavage fracture feature. Combined with the side surface in Fig. 10(a), it can be predicated that fracture occurred inside the solder close to the solder/Cu interface. The fracture mechanism of the as-soldered SnBi/Cu samples is slightly different. The macroscopic fracture surface of the SnBi/CuAg joints aged for 13 days

is shown in Fig. 10(c), in which a relatively smooth morphology is compared with that of the as-soldered samples. The microscopic morphologies on the two fracture surfaces are also different to some extent. As shown in Fig. 10(d), the fracture surface is the same as the bright region in the long-term aged SnBi/Cu joints; i.e., cleavage fracture occurred in the solder close to the  $\text{Cu}_6\text{Sn}_5$ /solder interface, whereas the brittle region [as in Figs. 9(b) and 9(c)] was never observed on the fracture surfaces of the SnBi/Cu–X samples even after aging for 20 days. It is implied that there is no essential transition in fracture mechanism of the SnBi/Cu–X solder joints during the aging process. The side surfaces shown in Fig. 9(c) also reveal that fracture still occurred inside the solder near the IMC/solder interface, only closer to the interface for the aged samples. Based on the interfacial microstructures and the tensile strength of the SnBi/Cu–X samples (Figs. 3 and 7), it can be concluded that the addition of Ag and Zn elements into Cu substrate has thoroughly eliminated the interfacial Bi embrittlement of the long-term aged Cu/ $\text{Cu}_3\text{Sn}$  interface under tensile loadings.

#### D. Fatigue property and fracture mechanism

It has been reported that the fatigue resistance of the SnBi/Cu interface was drastically weakened by aging, with a ductile-to-brittle transition of the fracture mechanism.<sup>8,9</sup> This gives rise to an open question whether the fatigue property of the SnBi/Cu–X solder joints is reliable. In this section, the fatigue lives ( $N_f$ ) of

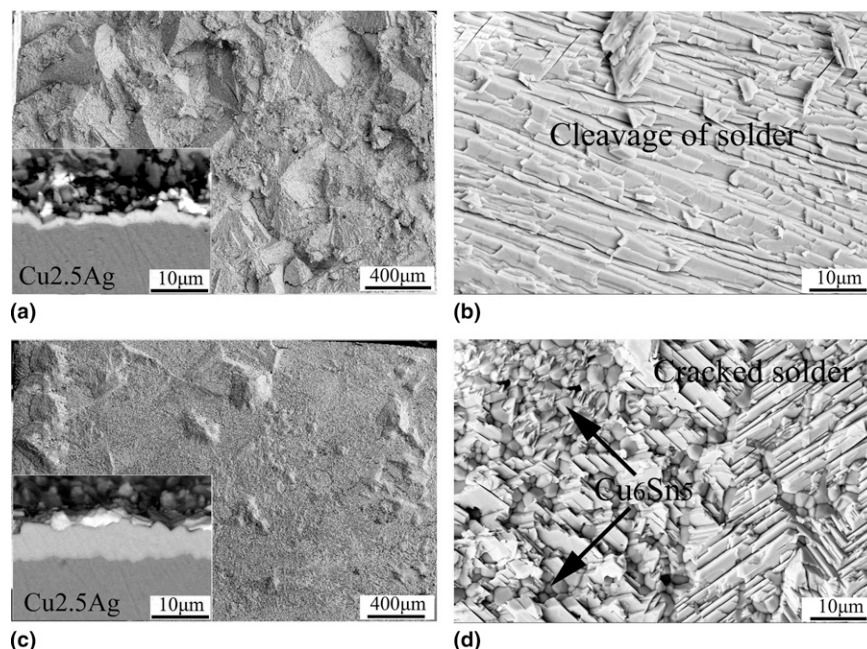


FIG. 10. Tensile fracture surfaces and side surfaces of SnBi/CuAg samples. (a) Macroscopic and (b) microscopic morphologies of the as-soldered samples. (c) Macroscopic and (d) microscopic morphologies of the aged samples.

the SnBi/Cu and SnBi/Cu–X solder joints under cyclic tension–compression loadings are examined and compared, then the fatigue fracture mechanisms are discussed to confirm the validity of Ag and Zn addition on keeping the fatigue resistance. Although the Sn–Bi alloy has a high strength and good elongation at low strain rate, some studies indicate that the fatigue property of the SnBi/Cu solder joint is inferior.<sup>3,29</sup> Therefore, the fatigue lives of the SnBi/Cu–X solder joints are also compared with that of the Sn–4Ag/Cu solder joints to make a full-scale evaluation of their fatigue resistance.

### 1. Fatigue lives of solder joints

The *S–N* relationships of the SnBi/Cu, Sn–4Ag/Cu, and SnBi/Cu–X solder joints aged for different times are shown in Fig. 11. To make a visual comparison, the fatigue lives of the SnBi/Cu and SnBi/Cu–X solder

joints aging for the same time are put together, and the scale of the coordinate in the four figures is the same. Fatigue lives of the as-soldered and samples aged for 7 days are shown in Figs. 11(a) and 11(b), respectively. It is found that the fatigue lives of the SnBi/Cu and SnBi/Cu–X joints are comparable but have slight differences; the SnBi/CuAg solder joints have longer fatigue lives than the SnBi/Cu samples, while those of the SnBi/CuZn solder joints are shorter. This phenomenon indicates that alloying Ag or Zn into the Cu substrate can affect the fatigue resistivity of the as-soldered SnBi/Cu joints, just like the influence on tensile strength, whereas the effect is not essential before the interfacial embrittlement occurs. After aging for 10 days, the SnBi/Cu solder joints became too brittle to carry out the fatigue test. In fact, they always fractured after a few cycles even at a stress amplitude of 20 MPa, exhibiting a brittle fracture and a sharp decrease in fatigue resistance. In contrast, the fatigue resistivities of the

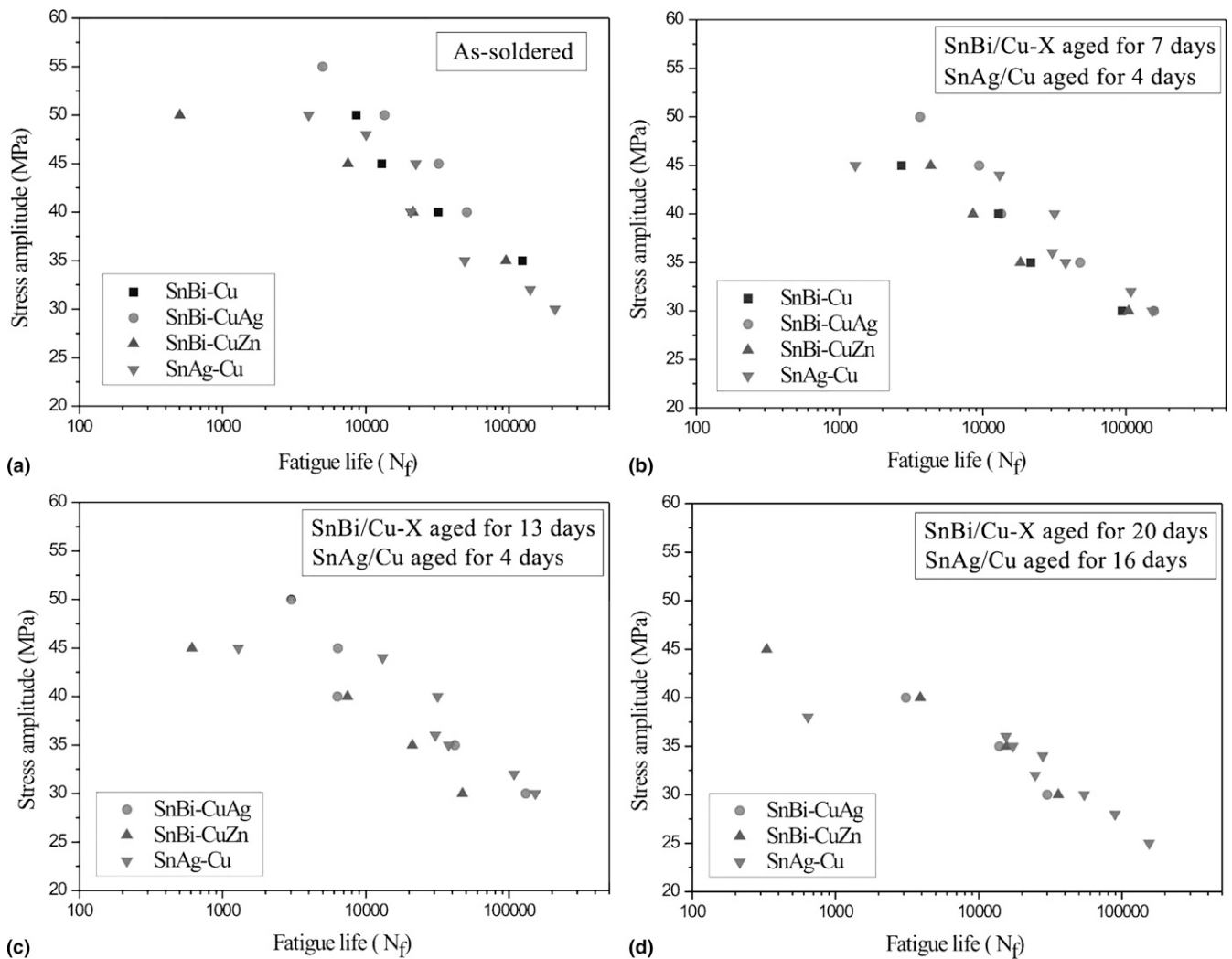


FIG. 11. *S–N* relationships of the SnBi/Cu, SnBi/Cu–X, and Sn–4Ag/Cu solder joints aged (at 120 °C for the former and 180 °C for the latter) for different times.



SnBi/Cu–X joint samples aged for 13 and 20 days are only slightly lower than those of the as-soldered joints. Therefore, it is predicated that the fatigue resistivity of the SnBi/Cu and the SnBi/Cu–X solder joints have similar evolution process with their tensile strength. The SnBi/Cu solder joints show a dramatic drop in fatigue resistivity once the interfacial Bi segregation appears, while the decrease in the fatigue resistivity of the SnBi/Cu–X solder joints is slight even after a long aged time (20 days).

The fatigue lives of the Sn–4Ag/Cu solder joints aged at 180 °C for different times are also shown in Fig. 11 for comparison. It is obvious that the data points of the SnBi/Cu–X and the Sn–4Ag/Cu solder joints in all the figures are approximately concurrent, indicating that their fatigue resistances are comparable under both the as-soldered and aged conditions. Although the deformability of the Sn–58Bi alloy is inferior at high strain rate, the tensile strength of the SnBi/Cu–X is much higher than the SnAg/Cu joints; thus the stress ratio ( $\sigma_a/\sigma_b$ ) of the former is much lower than the latter at the same stress amplitude. The higher tensile strength of the SnBi/Cu–X solder joints can therefore conceal their shortage to some extent, making their fatigue resistance comparable with that of the SnAg/Cu solder joints. Accordingly, as the SnAg solders are the most frequently used in electronic assembly and the fatigue lives of the SnAg/Cu joints can be used as a reference value, the aforementioned comparison also proves the

fatigue resistivity of the SnBi/Cu–X solder joints is reliable.

## 2. Fatigue fracture mechanisms

The fatigue behaviors of the SnBi/Cu–X and the SnBi/Cu solder joints are also quite similar before the interfacial embrittlement occurs. Therefore, we selected the SnBi/CuAg solder joints as an example to give a general description of the fatigue damage mechanisms. The interfacial deformation behavior and fatigue fracture surfaces of the aged SnBi/CuAg solder joints are exhibited in Fig. 12. Figure 12(a) shows the interfacial morphology of an as-soldered sample fatigued at a stress amplitude of 40 MPa for  $4 \times 10^4$  cycles. As shown in the figure, it seems that although the total plastic strain carried by the SnBi solder in the joint is small, the plastic deformation of the solders near the solder/IMC interface is a bit severe and microcracks were observed there. Because of the difference in the mechanical properties of the solder and the thin interfacial IMC layer, there is strain mismatch between them, leading to a severe strain localization near the interface.<sup>20</sup> Therefore, the interface is a weakness and becomes the crack initiation site. For the aged samples, the strain mismatch is much severe because the IMC layer is much thicker. Figure 12(b) shows the interfacial morphology of the sample aged for 13 days and tested at the stress amplitude of 35 MPa for  $2 \times 10^4$  cycles, in which the fatigue

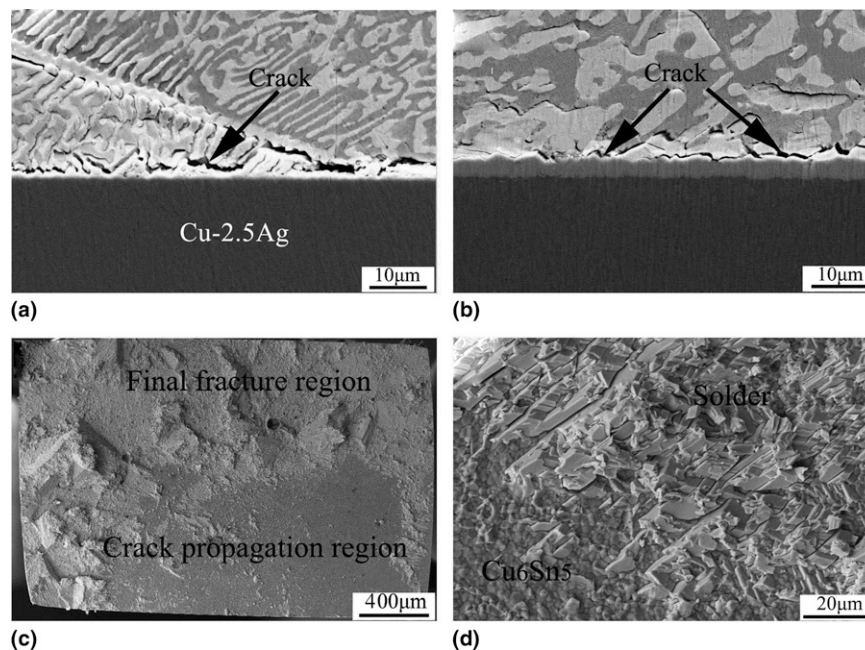


FIG. 12. Fatigue fracture surfaces of the SnBi/CuAg interfaces during cyclic loading. (a) Side surface morphologies of the as-soldered samples deformed at stress amplitude of 40 MPa for  $4 \times 10^4$  cycles (b) and samples aged for 13 days tested at 35 MPa for  $2 \times 10^4$  cycles. Fatigue fracture surfaces of the SnBi/CuAg samples aged for 13 days. (c) Macroscopic morphology. (d) Interface of crack propagation region and final fracture region.

cracks initiated exactly along the solder/Cu<sub>6</sub>Sn<sub>5</sub> interface. The fatigue fracture surfaces of the SnBi/Cu–X joint samples are also similar. Figure 12(c) shows the macroscopic fatigue fracture surface of the aged SnBi/CuAg joints, which is composed of two regions. The first region is covered by a thin layer of cracked solder, with Cu<sub>6</sub>Sn<sub>5</sub> grains under it [see Fig. 12(d)], similar to that of the tensile fracture surfaces of the aged samples. Therefore, it is considered to be the final fracture region and the first is the crack propagation region. In contrast, the second region is covered by perfect Cu<sub>6</sub>Sn<sub>5</sub> grains, with little residual solder. In comparison with Fig. 12(b), it is affirmed to be the crack propagation region. Based on the foresaid observations, it is predicated that the fatigue crack initiated at and propagated along the solder/Cu<sub>6</sub>Sn<sub>5</sub> interface as a result of strain localization, and finally fractured inside the solder near the interface.

The fatigue fracture mechanism of the as-soldered SnBi/Cu joint is similar to that of the SnBi/Cu–X joints. However, the long-term aged SnBi/Cu interface fractured along the Cu/Cu<sub>3</sub>Sn interface rapidly at low stress amplitude, and the fatigue fracture behavior is similar to its tensile fracture.<sup>30</sup> The long-term aged SnBi/Cu solder

joints under cyclic load parallel to the solder/Cu interface also fractured at the IMC/Cu interface rapidly.<sup>9</sup> In contrast, the fatigue fracture mechanisms of the as-soldered and the long-term aged SnBi/Cu–X samples are slightly different, as discussed previously; the decrease in fatigue resistance is also slight. Thus, it is confirmed that adding some Ag or Zn elements into the Cu substrate can effectively prevent interfacial embrittlement and keep the fatigue resistance of the SnBi/Cu–X solder joints reliable even after long-term aging.

According to the aforementioned experimental results and analyses, the influences of substrate alloying on the tensile strength, fatigue resistivity, and fracture mechanisms of the SnBi/Cu solder joints are summarized in Fig. 13. There is Bi segregation at the long-term aged Cu<sub>3</sub>Sn/Cu interface of the SnBi/Cu solder joints, which induced local brittle cracking of the solder joints under both tensile and fatigue loadings. Adding small amounts of Ag or Zn elements into the Cu substrate can thoroughly eliminate the interfacial Bi segregation even after long-term aging. Beyond that, there is no ductile-to-brittle transition in fracture mechanism for the SnBi/Cu–X solder joints during the aging process. The interfacial bonding strength and fatigue resistance of the

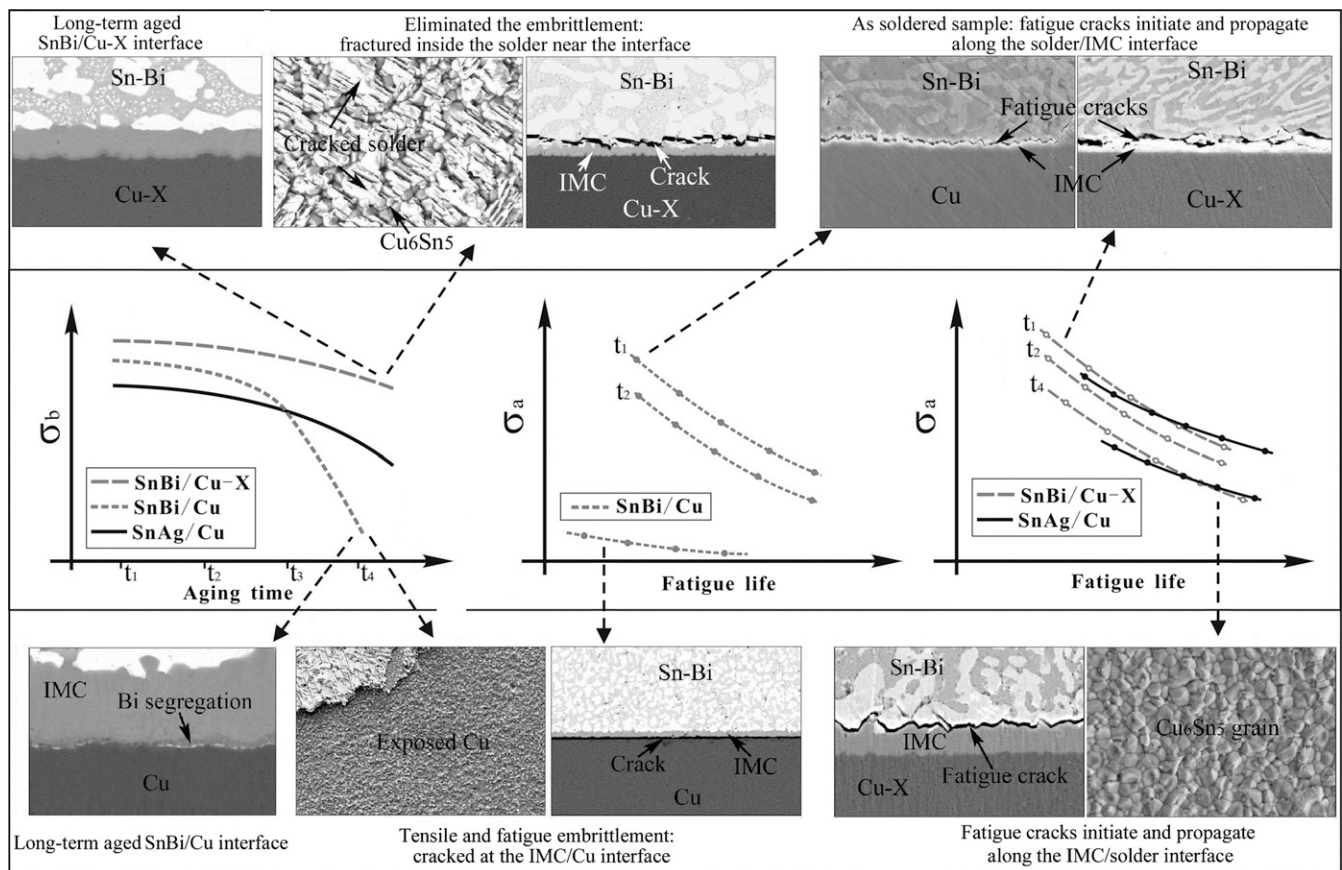


FIG. 13. Influence of substrate alloying on the tensile and fatigue properties and fracture behaviors of SnBi/Cu and SnBi/Cu–X solder joints.

long-term aged SnBi/Cu joint are maintained, indicating that the interfacial embrittlement has been healed. In comparison with the SnAg/Cu joints, the SnBi/Cu–X solder joints have higher adhesive strength and comparable fatigue resistivity, making the SnBi/Cu–X couples reliable in application. Because of its great effect to heal the interfacial Bi segregation and embrittlement problem of the SnBi/Cu solder joints, the substrate alloying techniques pave a potential way to the wide application for the SnBi alloy and other Bi-contained solders in the future.

#### IV. CONCLUSIONS

The interfacial morphology, tensile strength, fatigue lives, and fracture behaviors of the SnBi/Cu–X solder joints aged at 120 °C for different times have been investigated systematically and compared with those of the SnBi/Cu and Sn–4Ag/Cu joints. Based on the results and discussions in this article, the following conclusions can be drawn:

(1) A small quantity addition of Ag and Zn elements into the Cu substrate can restrain the Bi segregation at the SnBi/Cu interface during the aging process by accelerating Bi atoms to diffuse into the Cu–X alloy. The UTS of the SnBi/Cu–X solder joints is higher than that of the SnBi/Cu joints and only slightly decreases after long-term aging. Fracture of both the as-soldered and long-term aged SnBi/Cu–X joint samples occurred inside the solder approximate to the solder/IMC interface, confirming that the interfacial Bi embrittlement of the long-term aged SnBi/Cu–X interface has been eliminated.

(2) With increasing the aging time, the fatigue crack growth path of the SnBi/Cu interface changed from the solder/Cu<sub>6</sub>Sn<sub>5</sub> interface to the Cu<sub>3</sub>Sn/Cu interface, which drastically deteriorates the fatigue resistance of the SnBi/Cu joints, while such transition of the crack path was not observed at the SnBi/Cu–X interface and the fatigue resistance is maintained.

(3) Once eliminating the Bi segregation at the Cu/Cu–Sn IMC interface, the adhesive strength and fatigue resistivity of the long-term aged SnBi/Cu–X solder joints are reliable and comparable with those in the other Cu/lead-free solder joints. Thus, it is suggested that alloying Cu substrate with Ag or Zn element is a potential method to widely apply the Sn–Bi solder safely in the future.

#### ACKNOWLEDGMENTS

The authors would like to acknowledge Q.Q. Duan, P. Zhang, X.H. An, Y.Z. Tian, S. Qu, H.H. Su, L.X. Zhang, and W. Gao for sample preparation, tensile tests, and SEM observations. This work was financially supported

by National Basic Research Program of China under Grant No. 2010CB631006, the National Outstanding Young Scientist Foundation under Grant No. 50625103.

#### REFERENCES

1. S.K. Kang and A.K. Sarkhel: Lead (Pb)-free solders for electronic packaging. *J. Electron. Mater.* **23**, 701 (1994).
2. M. Abtew and G. Selvaduray: Lead-free solders in microelectronics. *Mater. Sci. Eng., R* **27**, 95 (2000).
3. Z. Mei and J.W. Morris Jr.: Characterization of eutectic Sn–Bi solder joints. *J. Electron. Mater.* **21**, 599 (1992).
4. J. Glazer: Microstructure and mechanical properties of Pb-free solder alloys for low-cost electronic assembly. A review. *J. Electron. Mater.* **23**, 693 (1994).
5. S. Smernos and R. Strauss: Low-temperature soldering. *Electrochem. Commun.* **57**, 148 (1982).
6. Z. Mei, F. Hua, J. Glazer, and C.C. Key: Low temperature soldering, in *21st IEEE/CPMT International Electronics Manufacturing Technology Symposium Proceedings* (IEMT Symposium, Austin, TX, 1997), p. 463.
7. P.L. Liu and J.K. Shang: Interfacial segregation of bismuth in copper/tin–bismuth solder interconnect. *Scr. Mater.* **44**, 1019 (2001).
8. P.L. Liu and J.K. Shang: Interfacial embrittlement by bismuth segregation in copper/tin–bismuth Pb-free solder interconnect. *J. Mater. Res.* **16**, 1651 (2001).
9. Q.S. Zhu, Z.F. Zhang, Z.G. Wang, and J.K. Shang: Inhibition of interfacial embrittlement at SnBi/Cu single crystal by electrodeposited Ag film. *J. Mater. Res.* **23**, 78 (2008).
10. P.L. Liu and J.K. Shang: Fracture of SnBi/Ni(P) interfaces. *J. Mater. Res.* **20**, 818 (2005).
11. H.F. Zou, Q.K. Zhang, and Z.F. Zhang: Eliminating interfacial segregation and embrittlement of bismuth in SnBi/Cu joint by alloying Cu substrate. *Scr. Mater.* **61**, 308 (2009).
12. V.J. Keast, A.L. Fontaine, and J.D. Plessis: Variability in the segregation of bismuth between grain boundaries in copper. *Acta Mater.* **55**, 5149 (2007).
13. G. Duscher, M.F. Chisholm, U. Alber, and M. Rühle: Bismuth-induced embrittlement of copper grain boundaries. *Nat. Mater.* **3**, 621 (2004).
14. R. Schweinfest, A.T. Paxton, and M.W. Finnis: Bismuth embrittlement of copper is an atomic size effect. *Nature* **432**, 1008 (2004).
15. S.Q. Liu and W.Q. Sun: Liquids of Ag–Cu–Bi system. *Acta Metall. Sinica* **24**, 376 (1988).
16. X. Deng, G. Piotrowski, J.J. Williams, and N. Chawla: Influence of initial morphology and thickness of Cu<sub>6</sub>Sn<sub>5</sub> and Cu<sub>3</sub>Sn intermetallics on growth and evolution during thermal aging of Sn–Ag solder/Cu joints. *J. Electron. Mater.* **32**, 1403 (2003).
17. M. He, Z. Chen, and G.J. Qi: Solid state interfacial reaction of Sn–37Pb and Sn–3.5Ag solders with Ni–P under bump metallization. *Acta Mater.* **52**, 2047 (2004).
18. J.W. Yoon, J.H. Lim, H.J. Lee, J. Joo, S.B. Jung, and W.C. Moon: Interfacial reactions and joint strength of Sn–37Pb and Sn–3.5Ag solders with immersion Ag-plated Cu substrate during aging at 150 °C. *J. Mater. Res.* **21**, 3196 (2006).
19. H.F. Zou, Q.K. Zhang, H.J. Yang, and Z.F. Zhang: *Mater. Sci. Eng., A* (2010, in press).
20. H.T. Lee, M.H. Chen, H.M. Jao, and T.L. Liao: Influence of interfacial intermetallic compound on fracture behavior of solder joints. *Mater. Sci. Eng., A* **358**, 134 (2003).
21. H.F. Zou and Z.F. Zhang: Ductile-to-brittle transition induced by increasing strain rate in Sn–3Cu/Cu joints. *J. Mater. Res.* **23**, 1614 (2008).

22. J.W. Yoon and S.B. Jung: Interfacial reactions and shear strength on Cu and electrolytic Au/Ni metallization with Sn–Zn solder. *J. Mater. Res.* **21**, 1590 (2006).
23. P.J. Shang, Z.Q. Liu, D.X. Li, and J.K. Shang: TEM observations of the growth of intermetallic compounds at the SnBi/Cu interface. *J. Electron. Mater.* **38**, 2579 (2009).
24. K. Tojima: *Wetting Characteristics of Lead-Free Solders*, Senior Project Report (Materials Engineering Department, San Jose State University, 1999).
25. Y. Yamagishi, M. Ochiai, H. Ueda, T. Nakanishi, and M. Kitazima: Pb-free solder of Sn-58Bi improved with Ag, in *Proceedings of the Ninth International Microelectronics Conference* (Omiya, Japan, 1996), p. 252.
26. Q.K. Zhang and Z.F. Zhang: unpublished work.
27. Q.K. Zhang and Z.F. Zhang: Fracture mechanism and strength-influencing factors of Cu/Sn–4Ag solder joints aged for different times. *J. Alloys Compd.* **485**, 853 (2009).
28. P.J. Shang, Z.Q. Liu, D.X. Li, and J.K. Shang: Bi-induced voids at the Cu<sub>3</sub>Sn/Cu interface in eutectic SnBi/Cu solder joints. *Scr. Mater.* **58**, 409 (2008).
29. W.J. Tomlinson and I. Collier: The mechanical properties and microstructures of copper and brass joints soldered with eutectic tin bismuth solder. *J. Mater. Sci.* **22**, 1835 (1987).
30. Q.K. Zhang, Q.S. Zhu, H.F. Zou, and Z.F. Zhang: Fatigue fracture mechanisms of Cu/lead-free solders interfaces. *Mater. Sci. Eng. A* (2009; DOI: 10.1016/j.msea.2009.10.040).